

---

# Multi-Stage Manipulation with Demonstration-Augmented Reward, Policy, and World Model Learning

---

Adrià López Escoriza<sup>1,2</sup> Nicklas Hansen<sup>1</sup> Stone Tao<sup>1,3</sup> Tongzhou Mu<sup>1</sup> Hao Su<sup>1,3</sup>

## Abstract

Long-horizon tasks in robotic manipulation present significant challenges in reinforcement learning (RL) due to the difficulty of designing dense reward functions and effectively exploring the expansive state-action space. However, despite a lack of dense rewards, these tasks often have a multi-stage structure, which can be leveraged to decompose the overall objective into manageable subgoals. In this work, we propose Demonstration-Augmented Reward, Policy, and World Model Learning (DEMO<sup>3</sup>), a framework that exploits this structure for efficient learning from visual inputs. Specifically, our approach incorporates multi-stage dense reward learning, a bi-phasic training scheme, and world model learning into a carefully designed demonstration-augmented RL framework that strongly mitigates the challenge of exploration in long-horizon tasks. Our evaluations demonstrate that our method improves data-efficiency by an average of 40% and by 70% on particularly difficult tasks compared to state-of-the-art approaches. We validate this across 16 sparse-reward tasks spanning four domains, including challenging humanoid visual control tasks using as few as five demonstrations. Website with code and visualizations can be found at <https://adrialopezescoriza.github.io/demo3>.

## 1. Introduction

Reinforcement learning (RL) with dense rewards has enabled significant progress in high-dimensional control tasks. Many such tasks are now solvable when the reward function is carefully designed for the specific goal. In particular, model-based RL (MBRL) has demonstrated strong performance in these high-dimensional problems (Ha &

Schmidhuber, 2018; Zhang et al., 2018; Kidambi et al., 2020; Hafner et al., 2020; Yu et al., 2020; Hansen et al., 2022; 2024; Sferrazza et al., 2024). However, designing accurate reward functions is challenging. Poorly designed rewards can lead agents to become trapped in local minima or exploit unintended shortcuts, resulting in undesirable behaviors (Clark & Amodei, 2016). More critically, scaling reward design to complex tasks is highly impractical: the larger the state space and the longer the horizon, the more intricate the reward must be. While recent approaches leveraging Large Language Models (Kwon et al., 2023; Ma et al., 2023; Xie et al., 2024) and Vision-Language Models (Rocamonde et al., 2024; Baumli et al., 2024) for reward generation show promise, they still struggle with high-precision requirements, particularly in manipulation problems. In contrast, sparse rewards, such as binary signals indicating task or subtask completion, are much easier to obtain. However, traditional RL methods still struggle to learn effectively from sparse rewards.

Fortunately, long-horizon tasks do offer opportunities to simplify the problem. Typically, such tasks exhibit a natural multi-stage structure. For example, a pick-and-place task can be broken down into subtasks such as grasping, lifting, and placing. Each of these can be associated with stage indicators or rewards that can easily be queried from the environment. This multi-stage structure allows these tasks to be decomposed into more manageable subgoals, enabling the agent to collect rewards more frequently (Smith et al., 2020; Di Palo & Johns, 2021). However, subgoal sparse rewards can still be insufficient if the distance between subgoals is too great, leading back to the exploration problem.

Prior work shows that Learning from Demonstrations (LfD) helps mitigate exploration issues in sparse reward settings. Algorithms such as CoDER (Zhan et al., 2022) and MoDem (Hansen et al., 2023; Lancaster et al., 2024) leverage demonstrations to populate the replay buffer of an off-policy RL algorithm (Sutton & Barto, 2018), but they often scale poorly with task complexity as they need demonstrations that sufficiently cover the behavior space. Inverse RL methods (Trott et al., 2019; Wu et al., 2021; Memarian et al., 2021; Escontrela et al., 2022) train RL on a reward function that is learned from demonstrations, but inverse RL alone

<sup>1</sup>University of California San Diego <sup>2</sup>ETH Zürich, Switzerland <sup>3</sup>Hillbot. Correspondence to: Adrià López Escoriza <alopez@ethz.ch>.

Work done during an internship at the University of California San Diego.

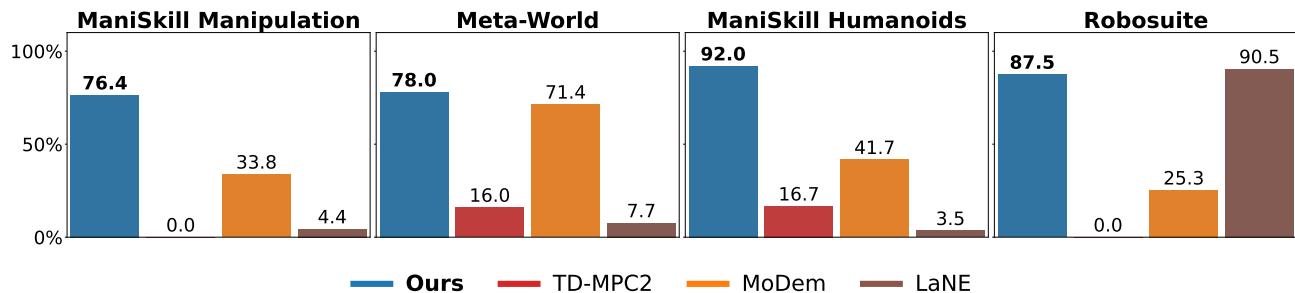


**Figure 1. Summary of results.** Final success rate (%) achieved by our method and a set of strong baselines, averaged across all tasks within each of 4 domains. Average of 5 seeds. Given a handful of demonstrations, our method achieves high success rates in challenging visual manipulation tasks with sparse rewards, far exceeding previous state-of-the-art methods. See Appendix A for per-task results.

often struggles as the learned reward function can have poor reward predictions on unseen states. Lastly, these methods typically require a vast amount of samples to learn a reward function (Kumar et al., 2022; Mu et al., 2024) before any policy learning can begin.

In this paper, we build on demonstration-augmented RL to tackle multi-stage manipulation tasks with sparse stage-wise rewards. We introduce DEMO<sup>3</sup>, a model-based RL algorithm that leverages a limited number of demonstrations for three key purposes: **learning a policy, a world model, and a dense reward**. DEMO<sup>3</sup> exploits the multi-stage structure of long-horizon tasks to transform sparse stage indicators into a stage-wise dense reward. This enables dense feedback in a structured way, prioritizing achieving subgoals over following demonstrations. Unlike prior work, our dense reward is learned online, alongside policy and world model learning.

We evaluate our method on a range of challenging manipulation tasks from Meta-World (Yu et al., 2021), Robosuite (Zhu et al., 2022), as well as both humanoid and tabletop manipulation tasks from ManiSkill3 (Tao et al., 2024b). Our results (see Figure 1) demonstrate that our method outperforms state-of-the-art methods by an average of 40%, and for more complex, longer-horizon tasks, this performance gap increases to 70%. **Our main contributions can be summarized as follows:**

1. We introduce DEMO<sup>3</sup>, an MBRL algorithm for highly data-efficient robotic manipulation from visual inputs and sparse rewards. Our method integrates online dense reward learning into RL for multi-stage tasks.
2. We conduct extensive experiments in 16 tasks across 4 domains to demonstrate the data-efficiency and robustness of our approach compared to existing methods.
3. We analyze the relative importance of each component of our framework, and are **committed to open-sourcing all code and demonstrations used in this work**.



**Figure 2. Task domains.** We evaluate methods on 16 multi-stage image-based sparse-reward tasks spanning four domains: Meta-World (Yu et al., 2021), Robosuite (Zhu et al., 2022), as well as manipulation and humanoid tasks from ManiSkill3 (Tao et al., 2024b). See Appendix D for a complete overview of tasks.

## 2. Preliminaries

**Problem formulation.** We aim to learn control policies for multi-stage, long-horizon tasks, which we model as infinite-horizon Markov Decision Processes (Bellman, 1957) defined by the tuple  $(\mathcal{S}, \mathcal{A}, \mathcal{P}, \mathcal{R}, \gamma)$ . Here,  $\mathcal{S}$  and  $\mathcal{A}$  denote the state and action spaces, respectively,  $\mathcal{P}$  is the (unknown) state transition probability function,  $\mathcal{R}$  is a sparse reward function, and  $\gamma \in [0, 1)$  is the discount factor. Our goal is to learn a policy  $\pi_\theta : \mathcal{S} \rightarrow \mathcal{A}$  parameterized by  $\theta$  that maximizes the expected cumulative reward (return) over an infinite time horizon, formalized as  $\max \mathbb{E}_{\pi_\theta} [\sum_{t=0}^{\infty} \gamma^t r_t]$ .

**Multi-stage sparse rewards.** In this work, we focus on *multi-stage* tasks where the overall objective can be decomposed into a sequence of  $N$  subgoals or stages. Stage indicators are often easy to obtain; for example, in manipulation tasks, it is straightforward to query whether the agent has grasped an object. We model the (sparse) reward as a stage indicator function  $r : \mathcal{S} \rightarrow \{1, 2, \dots, N\}$  that maps each state to its corresponding stage. We assume no access to any privileged information from the environment (e.g. object configurations), and instead consider *multi-modal observations*  $\mathbf{o} = (\mathbf{x}, \mathbf{q})$  where  $\mathbf{x}$  denotes raw RGB images coming from the agent’s cameras, and  $\mathbf{q}$  denotes the proprioceptive state of the robot. This constitutes realistic sensory inputs available in typical robotic platforms.

**TD-MPC2** (Hansen et al., 2022; 2024) is a model-based RL algorithm that combines Model Predictive Control (MPC), a

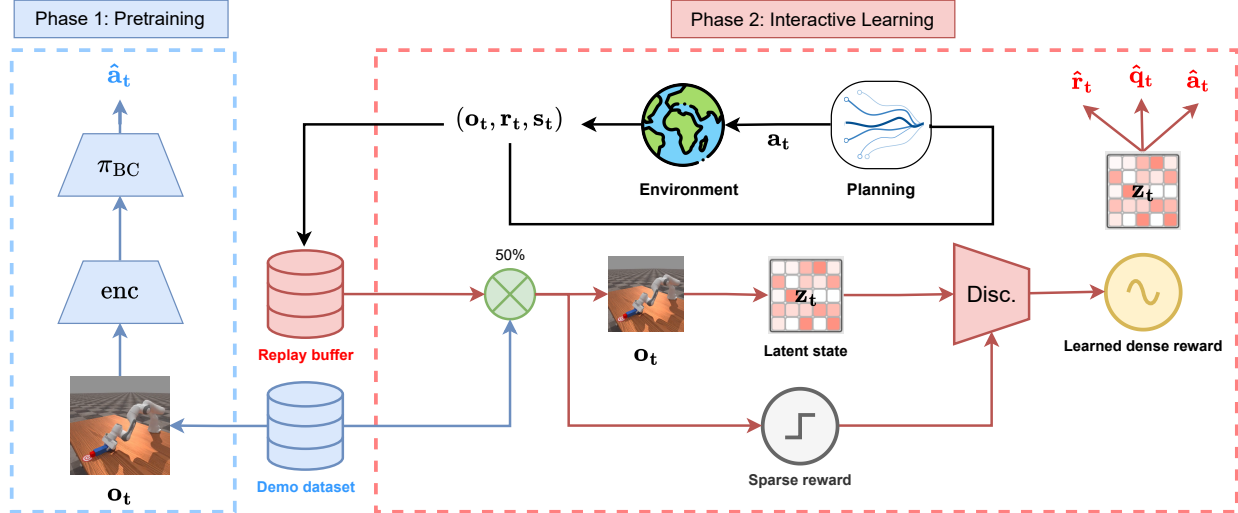


Figure 3. **Method overview.** We present a two-phase framework for multi-stage visual manipulation from sparse rewards that leverages a handful of demonstrations for dense reward learning and MBRL. **Phase 1 (left):** policy and encoder is pre-trained on the available demonstrations using behavioral cloning, which serve as initialization for the next phase. **Phase 2 (right):** the agent iteratively collects environment data via planning and uses all available data to update its world model as well as a latent state discriminator; this discriminator is used to transform sparse environment rewards into a learned dense reward for world model learning and subsequent planning.

learned latent-space world model, and a terminal value function learned via temporal difference (TD) learning. Specifically, TD-MPC2 learns a representation  $\mathbf{z} = h_\theta(\mathbf{o})$  that maps a high-dimensional observation  $\mathbf{o}$  into a compact representation  $\mathbf{z}$ , as well as a dynamics model in this latent space  $\mathbf{z}' = d_\theta(\mathbf{z}, \mathbf{a})$ . In addition, TD-MPC2 also learns prediction heads,  $R_\theta, Q_\theta, \pi_\theta$ , for (i) instantaneous reward  $r = R_\theta(\mathbf{z}, \mathbf{a})$ , (ii) state-action value  $Q_\theta(\mathbf{z}, \mathbf{a})$ , and (iii) a policy prior  $\mathbf{a} \sim \pi_\theta(\mathbf{z})$ . The policy prior  $\pi_\theta$  serves to “guide” planning towards high-return trajectories and is optimized to maximize temporally weighted  $Q$ -values. The remaining components are jointly optimized to minimize TD-errors, and reward and latent state prediction errors, minimizing

$$\mathcal{L}_{\text{TD-MPC}}(\theta) = \sum_{i=t}^{t+H} \lambda^{i-t} [\mathcal{L}_Q(\theta) + \mathcal{L}_R(\theta) + \mathcal{L}_h(\theta)], \quad (1)$$

where  $\mathbf{o}'_t, \mathbf{z}'_t$  are the (latent) states at time  $t+1$ . During environment interaction, TD-MPC2 selects actions via sample-based planner MPPI (Williams et al., 2015) and the learned world model. We adopt TD-MPC2 as our choice of visual MBRL algorithm due to its simplicity and strong empirical performance but emphasize that our framework can be instantiated with any MBRL algorithm.

### 3. Method

In this work, we address the challenge of solving multi-stage manipulation tasks from sparse rewards. Such long-horizon tasks are particularly difficult due to the combinatorial complexity of the state-action space and the lack of informative feedback across extended horizons. To overcome these is-

ues, we propose DEMO<sup>3</sup>, a novel RL method that uses demonstrations for a three-fold purpose: to learn a policy, a world model, and a dense reward simultaneously.

As our main algorithmic contribution, we introduce stage-specific reward learning. In particular, we extend the strategy on reward learning from demonstrations (LfD) presented in Mu et al. (2024) to online reward learning within a world model. By learning structured, multi-stage rewards online alongside world model and policy, our method provides more frequent and meaningful training signals to the agent than prior work on demonstration-augmented RL.

Our approach builds directly upon the strengths of prior work. In particular, we leverage MoDem’s multi-phase accelerated learning framework and use TD-MPC2 as our backbone for its robustness and generalizability.

#### 3.1. Model-based RL with online reward learning

Sparse rewards are a major challenge in RL, particularly for long-horizon tasks comprising multiple stages. To overcome this, we learn to densify sparse rewards with a small number of demonstrations. For this, we introduce a series of discriminators  $\{\delta_k\}_{k=0}^N$ , each corresponding to a task stage  $k \in \{0 \dots N\}$ . Each discriminator is trained to predict the likelihood of progressing to the next stage based on the latent state representation  $\mathbf{z}_t$  produced by the world model.

Therefore, each discriminator  $\delta_k$  acts as a **stage classifier** trained to distinguish states as either leading or not leading to successful stage transitions. For each stage  $k$ , we use a

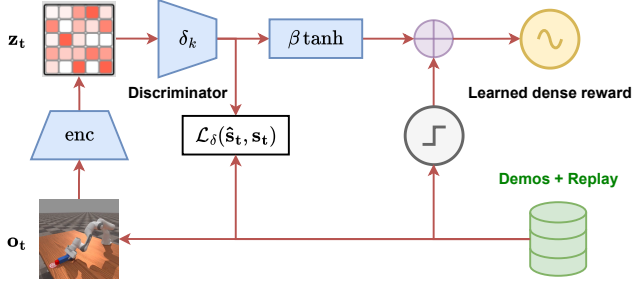


Figure 4. **Dense reward learning.** At each update step, the continuous output of a stage discriminator is added to the environment sparse reward. The discriminator output is normalized to the  $[-\beta, \beta]$  interval with a tanh operator.

typical Binary Cross Entropy (BCE) loss:

$$\mathcal{L}_{\delta_k} = \mathbb{E}_{(\mathbf{o}_t, r_t=k, s_t) \sim \mathcal{B}} [\text{BCE}(\mathbb{1}_{s_t > k}, \delta_k(\mathbf{h}(\mathbf{o}_t)))], \quad (2)$$

where  $\mathbf{h}$  denotes the world model encoder,  $\mathcal{B}$  is the replay buffer, and  $s_t$  represents the maximum stage that will be reached by the trajectory after the given sample:

$$s_t = \max_{t' \geq t} r_{t'}, \quad (3)$$

We refer to  $s_t$  as the *maximum stage label* of a sub-trajectory. Thus, each trajectory,  $\tau_i = \{(\mathbf{o}_t, \mathbf{a}_t, r_t, \mathbf{o}_{t+1}, s_t)\}_{t=0}^{T-1}$ , is annotated with *maximum stage labels*  $s_t$  that serve as success labels for the stage discriminators. Then, as presented in Algorithm 1, at each update of the world model, the discriminators are updated as an additional part of the model. Specifically, for a given sample from the replay buffer  $(\mathbf{o}_t, \mathbf{a}_t, \mathbf{o}_{t+1}, r_t, s_t) \sim \mathcal{B}$ , the sparse reward associated with a given stage,  $k = r_t$ , will tell us which discriminator,  $\delta_k$ , will be updated by that sample. If the *maximum stage label*  $s_t$  is greater than the current stage reward  $k = r_t$ , the sample belonging to a trajectory with a successful stage transition will be treated as a positive example in the classifier loss. Note that in the event that no samples with a stage reward,  $r_t = k$ , would appear in a given batch, the discriminator  $\delta_k$  for that stage would simply not get updated at that step. Therefore, while the algorithm is capable of working without any demonstrations, using a small demonstration dataset can significantly accelerate the training of the world model and discriminators.

While training the world model, the discriminators are used to **generate dense rewards** as per

$$\hat{r}_t^\delta = r_t + \beta \cdot \tanh(\delta_{r_t}(\mathbf{z}_t)) \quad (4)$$

where the output of the discriminator is mapped to the  $[-\beta, \beta]$  interval. The process is illustrated by Figure 4. We set  $\beta$  to be a hyperparameter with  $\beta \leq 1/3$  to ensure that rewards never cross between different stage regions.

### Algorithm 1 DEMO<sup>3</sup> (Phase 2)

**Require:** Demonstration dataset  $\mathcal{D}$ , number of stages  $N$

- 1: Initialize discriminators  $\{\delta_k\}_{k=0}^N$
- 2: Initialize replay buffer  $\mathcal{B} \leftarrow \{\emptyset\}$

#### Rollout

- 3: **for** each environment step **do**
- 4:   **if**  $\text{rand}() \geq \alpha$  **then**
- 5:     Agent step:  $\mathbf{a}_t \sim \pi_{\text{BC}}(\mathbf{a}|\mathbf{h}(\mathbf{o}_t))$
- 6:   **else**
- 7:     Agent step:  $\mathbf{a}_t \leftarrow \text{WM}_{\text{plan}}(\mathbf{o}_t)$
- 8:   **end if**
- 9:   Env step:  $(\mathbf{o}_{t+1}, r_t) \leftarrow \text{Env}(\mathbf{o}_t, \mathbf{a}_t)$
- 10:   Save sample:  $\tau \leftarrow \tau \cup (\mathbf{o}_t, \mathbf{a}_t, \mathbf{o}_{t+1}, r_t)$
- 11:   **if** episode done **then**
- 12:     Reset environment
- 13:     Compute maximum stage labels:  $\{s_t\}_0^T$
- 14:     Save trajectory:  $\mathcal{B} \leftarrow \mathcal{B} \cup (\tau \cup \{s_t\}_0^T)$
- 15:   **end if**
- 16:    $\alpha \leftarrow \min(1, \alpha_0 \cdot t)$
- 17: **end for**

#### Update

- 18: **for** each update step **do**
- 19:   Sample:  $\{(\mathbf{o}_t, \mathbf{o}_{t+1}, \mathbf{a}_t, r_t, s_t)_{t_0}^{t_0+H}\} \sim (\mathcal{B} \cup \mathcal{D})$
- 20:   Predict dense reward  $(\hat{r}_t^\delta)_{t_0}^{t_0+H}$
- 21:   Compute world model losses:  $\mathcal{L}_R, \mathcal{L}_Q, \mathcal{L}_h, \mathcal{L}_\pi$
- 22:   Compute discriminator loss:  $\mathcal{L}_\delta = \frac{1}{N} \sum_k \mathcal{L}_\delta^k$
- 23:   Gradient step:  $\theta \leftarrow \theta + \rho \nabla \mathcal{L}_P$
- 24: **end for**

This is to ensure that states belonging to a more advanced stage always get a higher reward than lower-stage states. Effectively, our method rewards states that have a higher chance of transitioning to the next stage and penalizes those that do not, encouraging the agent to explore regions with a higher probability of transition.

The total world model loss integrating these signals becomes

$$\mathcal{L}_P = \mathcal{L}_R + \mathcal{L}_Q + \mathcal{L}_h + \mathcal{L}_\delta, \quad (5)$$

where  $\mathcal{L}_R$ ,  $\mathcal{L}_Q$ , and  $\mathcal{L}_h$  represent the TD-MPC2 world model losses: (i) reconstruction, (ii) value estimation, and (iii) latent dynamics losses. Importantly,  $\mathcal{L}_R$  is computed to predict the learned dense reward produced by the discriminator,  $\hat{r}_t^\delta$ , thus providing a richer learning signal than pure sparse rewards. Finally,  $\mathcal{L}_\delta$  is the average loss of all the stage discriminators. As in Hansen et al. (2024), the total loss is used to compute gradients for the world model, meaning that  $\mathcal{L}_\delta$  is also used to learn the observation encoder.

### 3.2. Training scheme

In order to further boost the data-efficiency of DEMO<sup>3</sup>, we build upon previous work on accelerating MBRL with

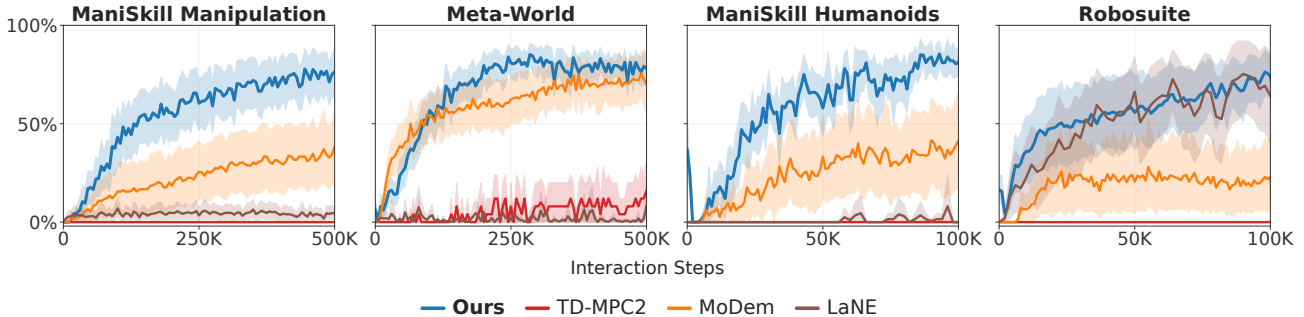


Figure 5. **Learning curves.** Success rate as a function of interaction steps for each of the four domains that we consider, averaged across all tasks and 5 random seeds. The shaded area corresponds to a 95% confidence interval. Our method consistently outperforms baselines.

demonstrations. Specifically, we draw inspiration from MoDem (Hansen et al., 2023) and propose a bi-phase training scheme in which we first use demonstrations to pre-train an initial policy through behavioral cloning (Atkeson & Schaal, 1997; Pomerleau, 1988),  $\pi_{BC}$  to collect informative samples during early stages of training. In phase 2, we gradually phase out the (frozen) pre-trained policy and start collecting samples by planning through the world model, which is learned via interactive learning. An overall diagram of our training strategy can be found in Figure 3.

**Phase 1: Pretraining.** One of the main bottlenecks of RL in long-horizon sparse reward tasks is the low-informative data that is collected at the early stages of training. As early data tends to contain no rewards, learning a meaningful representation for such states becomes challenging. Traditional methods tend to start collecting data with a randomly initialized policy that usually struggles to find any rewards in the environment. For this reason, we jointly pre-train a policy  $\pi_{BC}$  and an encoder  $h_{BC}$  on the full demonstration dataset  $\mathcal{D}$  using the classic behavioral cloning (BC) loss as an objective function:

$$\mathcal{L}_{BC}(\theta) = \mathbb{E}_{(\mathbf{o}, \mathbf{a}) \sim \mathcal{D}} [-\log \pi_{\theta}(\mathbf{a} | h_{\theta}(\mathbf{o}))], \quad (6)$$

where the policy learns to imitate the behaviors encoded in the dataset. At interaction time, the interactive policy  $\pi_{RL}$  and the world model encoder,  $h$ , are initialized with their pre-trained analogs  $\pi_{BC}$ ,  $h_{BC}$ .

Given that we focus on datasets with limited demonstrations, behavioral cloning can be prone to overfitting (Peters et al., 2010; Parisi et al., 2022; Duan et al., 2017). To mitigate this, we regularly evaluate  $\pi_{BC}$  during pretraining by rolling out episodes in the environment. We use early stopping on the evaluation set (Yao et al., 2007) to select the best-performing policy for the interactive learning phase.

**Phase 2: Interactive Learning.** After initial pretraining of the encoder and policy, the agent starts collecting data from the environment to learn using offline reinforcement learning (RL). In order to utilize the demonstrations, we

Table 1. **Experimental setup.** We consider 16 challenging visual manipulation tasks in 4 different domains. Domains that empirically present a slower convergence are given a bigger budget of interactions. The number of stages is determined according to the nature of the task and by the typical horizon of demonstrations.

Domain	Tasks	Demos	Interactions	Stages
<b>ManiSkill</b>	5	5-100	500k	3
<b>Meta-World</b>	5	5	500k	2
<b>Robosuite</b>	4	5-25	100k	1
<b>Humanoids</b>	2	5	100k	3

follow Hansen et al. (2023) by sampling from the replay buffer  $\mathcal{B}$  and the demonstration dataset  $\mathcal{D}$  at each update step. Specifically, every time we sample a batch, a fraction of the samples come from  $\mathcal{D}$  while the remaining fraction comes from  $\mathcal{B}$ . This approach prevents collected data from quickly outnumbering the demonstrations. While the sampling ratio is a tunable hyperparameter, we empirically found that an initial 50% demonstration ratio works well for most tasks.

Therefore, as detailed in Algorithm 1, at each update step, the world model gets updated as explained in Section 3.1. The agent will then proceed to interact with the environment to collect more data that will be stored in the replay buffer.

Similar to Lancaster et al. (2024), we use annealing to control the probability of a sample coming from  $\pi_{BC}$  or from the planning module of the world model. In this way, the data distribution of the replay buffer  $\mathcal{B}$  is initially biased toward the one of the dataset  $\mathcal{D}$ . This technique aims to collect more informative data than the one a purely random policy would collect during early stages of training. As the world model starts learning and  $\pi_{RL}$  is able to collect more meaningful samples, we increase the annealing coefficient  $\alpha_t$  to improve the diversity of collected samples and stop relying on the suboptimal pre-trained policy  $\pi_{BC}$ . Eventually,  $\alpha_t$  will converge to 1, at which point all samples will come from planning with  $\pi_{RL}$  (see Algorithm 1).

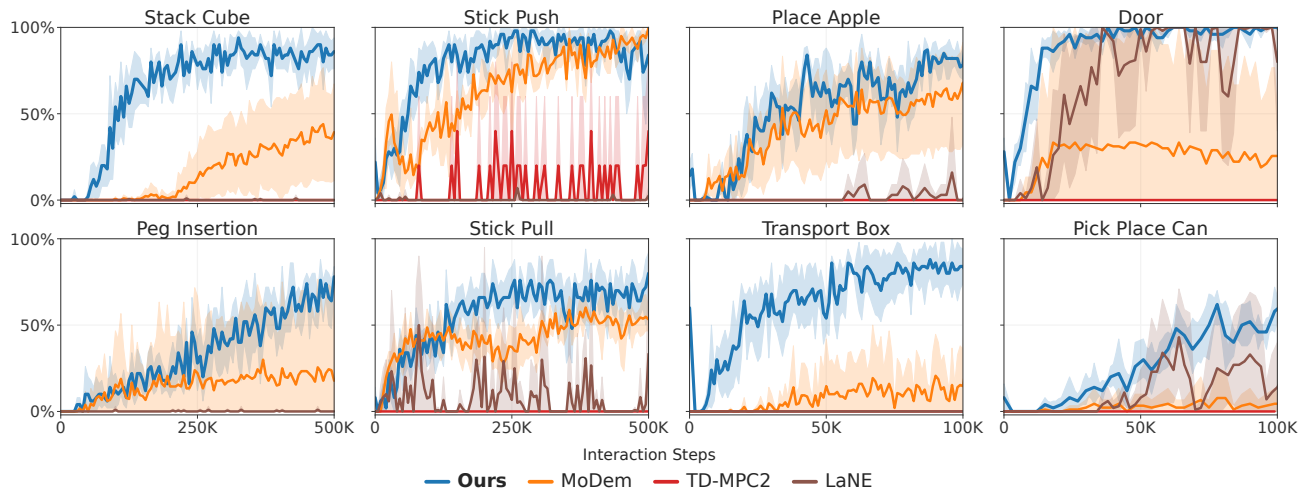


Figure 6. **Challenging tasks.** Success rate of our method and baselines on the 2 hardest tasks from each domain. Averaged across 5 random seeds. LaNE results in Robosuited are kindly provided by Zhao et al. (2024). Shaded areas correspond to 95% confidence intervals.

## 4. Experiments

We consider **16** challenging visual multi-stage manipulation tasks with a long-horizon for our experimental evaluation. This includes **5** manipulation tasks from *ManiSkill3* (Tao et al., 2024b), **5** manipulation tasks from *Meta-World* (Yu et al., 2021) and **4** manipulation tasks from *Robosuited* (Zhu et al., 2022). Additionally, we include **2** humanoid manipulation tasks from *ManiSkill3* with a high-dimensional action space, which we refer to as *ManiSkill Humanoids* in our evaluations. We place a strong emphasis on long-horizon precise manipulation, which is why we select the most challenging tasks from each domain. We relate the difficulty to the required precision of a task, its horizon, and the level of randomization in the scene (see Appendix D.3 for further details on difficulty categorization). For each task, the agent is given a constrained budget of demonstrations and interaction steps (see Table 1). To allow most baselines to solve the task, we set the interaction budget and demonstrations to a different amount for each task. For a complete list of details on our experimental setup, please refer to Table 1 and Appendix D. **We have open-sourced all code and environments**<sup>1</sup>. Through our evaluations, we aim to answer the following questions:

1. Can our proposed method effectively accelerate MBRL with demonstrations in long-horizon multi-stage tasks?
2. What is the relative importance of each algorithmic component of Demonstration-Augmented Reward, Policy, and World Model Learning (DEMO<sup>3</sup>), and how does it scale with the amount of demonstration data?
3. How do sparse reward functions compare to our learned rewards at different levels of stage granularity?

<sup>1</sup><https://github.com/adrialescoriza/demo3>

### 4.1. Baselines

To assess our method’s effectiveness, we compare it against three relevant approaches. A complete comparison of other methods can be found in Appendix B.

**MoDem** (Hansen et al., 2023) is an MBRL algorithm designed to enhance data-efficiency in visual control tasks with sparse rewards. Similarly to our method, MoDem employs a three-phase framework: policy pretraining, seeding, and interactive learning with oversampling of demonstration data. The authors show state-of-the-art performance on *Meta-World* and *Adroit* domains from visual inputs.

**LaNE** (Zhao et al., 2024) is a data-efficient model-free RL method for sparse-reward tasks from visual inputs. LaNE utilizes a pre-trained feature extractor to learn an embedding space and **rewards the agent for exploring regions near the demonstrations within this latent space**. The authors also show state-of-the-art data-efficiency in the *Robosuited* environment with a limited amount of demonstrations.

**TD-MPC2** (Hansen et al., 2022; 2024) is the state-of-the-art MBRL algorithm for control tasks. It combines temporal difference learning with model predictive control (MPC) and constitutes the backbone of our approach. Compared to TD-MPC, TD-MPC2 includes a series of algorithmic changes that improve robustness and scaling.

### 4.2. Benchmark Results

The main result of our evaluations (see Figure 5) compares the data-efficiency of our method against the proposed baselines. On average, our method achieves 40% better data-efficiency than the proposed baselines. Notably, in *ManiSkill3*, our most difficult domain, DEMO<sup>3</sup> averages a 75% success rate after only 500k steps, performing 50% better

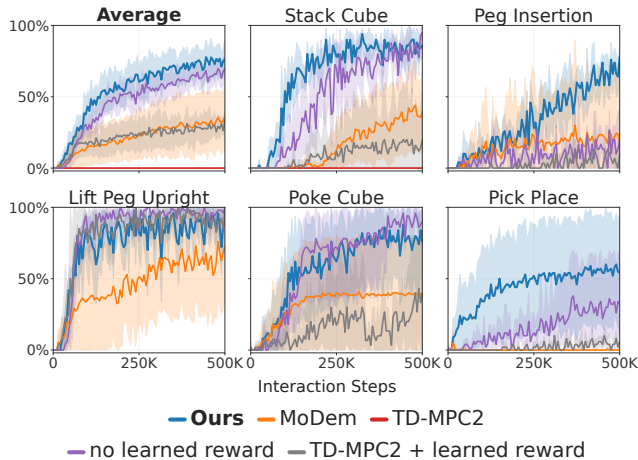


Figure 7. **Ablations.** Success rate as a function of interaction steps for variations of our method on all 5 ManiSkill manipulation tasks. Averaged across 5 random seeds. Baselines included for completeness. Shaded areas correspond to 95% confidence intervals.

than the second-best baseline. Furthermore, our DEMO<sup>3</sup> can deal better with the high-dimensional action space in ManiSkill Humanoids. Interestingly, while DEMO<sup>3</sup> does better on average, it thrives in tasks where the horizon and precision of the task are the highest. While the results of LaNE in the Robosuite domain are certainly impressive, the same approach doesn’t transfer to the rest of the domains.

Figure 6 shows the learning curves for the most challenging task of each benchmark. Particularly, the ManiSkill tasks, Peg Insertion, and Stack Cube, require a very high level of precision and a long horizon. As shown in 6, DEMO<sup>3</sup> is the only algorithm to reliably solve both tasks in the interaction budget. While performance is quite matched with LaNE (Zhao et al., 2024) in Robosuite, LaNE uses a pre-trained encoder to preprocess image observations while our method is completely learned from scratch. Finally, TD-MPC2 struggles to get any performance as is typical for pure RL algorithms learning from sparse rewards. Overall, DEMO<sup>3</sup> shows the highest degree of robustness and efficiency on the proposed long-horizon tasks.

### 4.3. Analysis

**Relative importance of each component** Figure 7 shows the effect of removing dense reward learning, policy pre-training, and demonstration oversampling in the 5 manipulation tasks from *ManiSkill3*. Interestingly, a considerable jump in performance is brought by pretraining and oversampling from the demonstration dataset with the TD-MPC2 backbone (*no learned reward*). The effect of reward learning becomes evident in long-horizon tasks where advancing stages can be very challenging without rewards (e.g., Peg Insertion, Pick Place), especially when reducing the number of demonstrations (see Appendix A.2).

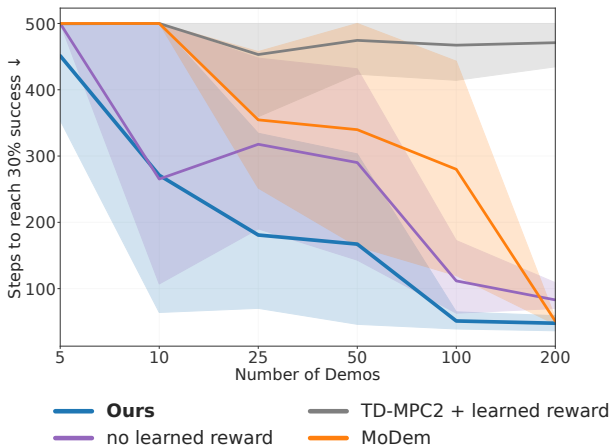


Figure 8. **Demonstration efficiency.** Number of steps to reach a critical success rate (30%) as a function of demonstration count. Data points that did not converge are assigned a 500k step count. Results are aggregated over 2 challenging manipulation tasks (Stack Cube and Peg Insertion) and averaged across 5 seeds. Shaded areas correspond to a 95% confidence interval.

**Demonstration efficiency** In Figure 8, we experiment with different dataset sizes and evaluate the data-efficiency of different baselines using demonstrations. While most methods scale well with the number of demonstrations, DEMO<sup>3</sup> shows the strongest performance in the lowest regime of demonstrations. This is particularly evident in challenging tasks such as Peg Insertion and Stack Cube, where DEMO<sup>3</sup> is the only method capable of reaching meaningful performance within the interaction budget (see Appendix A.2) with only 5 demonstrations.

**Wall-time comparison** Our method achieves competitive wall-time performance, ranking as the second fastest among all evaluated algorithms (Table 2). While slightly slower than TD-MPC2, we attribute the overhead to the additional computation required for reward learning. Importantly, DEMO<sup>3</sup> performs much faster than other demonstration-augmented RL approaches, such as Modem and LaNE.

Table 2. **Wall-time.** Hours per 100k interaction steps, averaged across 5 seeds and all tasks in Robosuite. Lower is better ↓.

Algorithm	Time (hours) ↓
LaNE	20.40
MoDem	8.37
TD-MPC2	<b>4.84</b>
Ours	5.19

**Reward granularity** Figure 9 illustrates the data-efficiency of our method across the same tasks under varying reward granularities: 1 stage, 2 stages, 3 stages, and dense

rewards. Please refer to D for details about the stage definitions. As expected, dense rewards provide the optimal learning signal, resulting in the fastest task completion. Remarkably, our method achieves near-equal performance with only 2 stages, demonstrating that stage indicators combined with a minimal set of demonstrations are sufficient to guide the learning process effectively. This result shows that over-engineered dense reward functions can easily be avoided by only providing a small amount of demonstrations. By relying solely on stage indicators and demonstrations, our method simplifies the reward design process while maintaining high performance in complex long-horizon tasks.

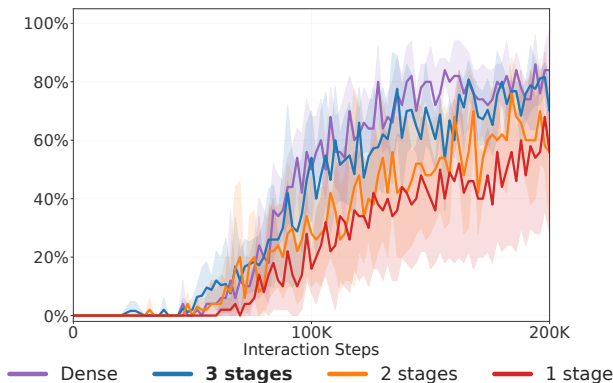


Figure 9. **Reward granularity.** Success rate of our method with increasing granularity in the stage division of a task. Results are aggregated over 2 challenging manipulation tasks (Stack Cube and Peg Insertion) and averaged across 5 seeds. The shaded area corresponds to a 95% confidence interval.

## 5. Related work

**Model-based RL** Model-based Reinforcement Learning (MBRL) improves data-efficiency by leveraging a model of the environment to guide decision-making. These models can be either prior-based, such as physics-based simulators, or learned, where the agent approximates a dynamic model of the world from data. World models (Schmidhuber, 1990; Ha & Schmidhuber, 2018) are an internal representation of the environment that enables planning and policy learning without direct interaction. A notable example is MuZero (Schrittwieser et al., 2020), which extends value-based planning by implicitly learning environment dynamics. Recent advances, such as Dreamer (Hafner et al., 2020; 2022; 2024) and TD-MPC (Hansen et al., 2022; 2024), improve learning in high-dimensional spaces, allowing MBRL to scale to complex visual and continuous control tasks.

**Demonstration-Augmented RL** Learning policies purely through trial and error can be inefficient and unstable, prompting research into leveraging demonstrations to enhance RL. During online interactions, demonstrations can serve as off-policy experience (Hester et al., 2018; Kaptur-

owski et al., 2018; Ball et al., 2023; Nair et al., 2018; Escontrela et al., 2022) or for on-policy regularization (Kang et al., 2018; Rajeswaran et al., 2017). Alternatively, demonstrations can be used to estimate reward functions for RL (Xie et al., 2018; Aytar et al., 2018; Vecerik et al., 2019; Zolna et al., 2020; Singh et al., 2019). *In this work, we leverage demonstrations in multiple ways simultaneously: learning an initial policy, the world model, and a reward function.*

**Reward Learning** Designing rewards is challenging due to the need for extensive domain knowledge, prompting the development of data-driven reward learning methods. Rewards can be learned from offline datasets by classifying goals (Smith et al., 2019; Kalashnikov et al., 2021; Du et al., 2023) or estimating goal distances (Zakka et al., 2022). Alternatively, inverse RL approaches (Ng et al., 2000; Ziebart et al., 2008; Ho & Ermon, 2016; Fu et al., 2017) leverage online interactions to infer a reward function from expert demonstrations. Additionally, reward shaping techniques (Trott et al., 2019; Wu et al., 2021; Memarian et al., 2021; Escontrela et al., 2022) transform sparse rewards into dense rewards using specific domain knowledge. The reward learning in this work builds upon DrS (Mu et al., 2024), with modifications tailored for compatibility with MBRL.

## 6. Conclusions and Future Directions

In this work, we address the challenge of learning long-horizon manipulation skills with sparse rewards using only proprioceptive and visual feedback. We propose DEMO<sup>3</sup>, a demonstration-augmented MBRL algorithm that simultaneously learns a reward function, policy, and world model for multi-stage manipulation tasks. Our experiments (see Section 4) show that DEMO<sup>3</sup> outperforms the state-of-the-art by 40% and converges 4× faster on the most difficult tasks.

Regarding future work, we identify two key directions. First, while our results indicate that a very small number of demonstrations is sufficient for accelerated learning, we do not investigate the impact of different demonstration sources, *e.g.*, human teleoperation. Although prior work suggests that such variations have a minor effect on RL performance (Hansen et al., 2023), making demonstration-augmented RL methods like DEMO<sup>3</sup> more robust to diverse data sources remains a valuable research direction.

Second, the integration of demonstrations within the MBRL framework warrants further exploration. Our results show that a simple 50% sampling schedule between demonstrations and the replay buffer already provides substantial benefits. This raises the question of whether more advanced sampling strategies could further improve data efficiency. Inspired by prioritized replay buffers (Schaul et al., 2016), optimizing demonstration sampling to maximize learning efficiency presents a promising avenue for future research.



## References

- Atkeson, C. G. and Schaal, S. Robot learning from demonstration. In *Proceedings of the Fourteenth International Conference on Machine Learning, ICML '97*, pp. 12–20, San Francisco, CA, USA, 1997. Morgan Kaufmann Publishers Inc. ISBN 1558604863.
- Aytar, Y., Pfaff, T., Budden, D., Paine, T., Wang, Z., and De Freitas, N. Playing hard exploration games by watching youtube. *Advances in neural information processing systems*, 31, 2018.
- Ball, P. J., Smith, L., Kostrikov, I., and Levine, S. Efficient online reinforcement learning with offline data. In *International Conference on Machine Learning*, pp. 1577–1594. PMLR, 2023.
- Baumli, K., Baveja, S., Behbahani, F., Chan, H., Comanici, G., Flennerhag, S., Gazeau, M., Holsheimer, K., Horgan, D., Laskin, M., Lyle, C., Masoom, H., McKinney, K., Mnih, V., Neitz, A., Nikulin, D., Pardo, F., Parker-Holder, J., Quan, J., Rocktäschel, T., Sahni, H., Schaul, T., Schroecker, Y., Spencer, S., Steigerwald, R., Wang, L., and Zhang, L. Vision-language models as a source of rewards, 2024. URL <https://arxiv.org/abs/2312.09187>.
- Bellman, R. A markovian decision process. *Indiana Univ. Math. J.*, 6:679–684, 1957. ISSN 0022-2518.
- Clark, J. and Amodei, D. Faulty reward functions in the wild. *OpenAI Blog*, 2016.
- Di Palo, N. and Johns, E. Learning multi-stage tasks with one demonstration via self-replay. In *Conference on Robot Learning (CoRL)*, 2021.
- Du, Y., Konyushkova, K., Denil, M., Raju, A., Landon, J., Hill, F., de Freitas, N., and Cabi, S. Vision-language models as success detectors. *arXiv preprint arXiv:2303.07280*, 2023.
- Duan, Y., Andrychowicz, M., Stadie, B. C., Ho, J., Schneider, J., Sutskever, I., Abbeel, P., and Zaremba, W. One-shot imitation learning, 2017. URL <https://arxiv.org/abs/1703.07326>.
- Escontrela, A., Peng, X. B., Yu, W., Zhang, T., Iscen, A., Goldberg, K., and Abbeel, P. Adversarial motion priors make good substitutes for complex reward functions, 2022. URL <https://arxiv.org/abs/2203.15103>.
- Fu, J., Luo, K., and Levine, S. Learning robust rewards with adversarial inverse reinforcement learning. *arXiv preprint arXiv:1710.11248*, 2017.
- Ha, D. and Schmidhuber, J. World models. 2018. doi: 10.5281/ZENODO.1207631. URL <https://zenodo.org/record/1207631>.
- Hafner, D., Lillicrap, T., Ba, J., and Norouzi, M. Dream to control: Learning behaviors by latent imagination, 2020. URL <https://arxiv.org/abs/1912.01603>.
- Hafner, D., Lillicrap, T., Norouzi, M., and Ba, J. Mastering atari with discrete world models, 2022. URL <https://arxiv.org/abs/2010.02193>.
- Hafner, D., Pasukonis, J., Ba, J., and Lillicrap, T. Mastering diverse domains through world models, 2024. URL <https://arxiv.org/abs/2301.04104>.
- Hansen, N., Wang, X., and Su, H. Temporal difference learning for model predictive control. In *ICML*, 2022.
- Hansen, N., Lin, Y., Su, H., Wang, X., Kumar, V., and Rajeswaran, A. Modem: Accelerating visual model-based reinforcement learning with demonstrations. 2023.
- Hansen, N., Su, H., and Wang, X. Td-mpc2: Scalable, robust world models for continuous control, 2024.
- Hester, T., Vecerik, M., Pietquin, O., Lanctot, M., Schaul, T., Piot, B., Horgan, D., Quan, J., Sendonaris, A., Osband, I., et al. Deep q-learning from demonstrations. In *Proceedings of the AAAI Conference on Artificial Intelligence*, volume 32, 2018.
- Ho, J. and Ermon, S. Generative adversarial imitation learning. *Advances in neural information processing systems*, 29, 2016.
- Kalashnikov, D., Varley, J., Chebotar, Y., Swanson, B., Jonschkowski, R., Finn, C., Levine, S., and Hausman, K. Mt-opt: Continuous multi-task robotic reinforcement learning at scale. *arXiv preprint arXiv:2104.08212*, 2021.
- Kang, B., Jie, Z., and Feng, J. Policy optimization with demonstrations. In *International conference on machine learning*, pp. 2469–2478. PMLR, 2018.
- Kapturowski, S., Ostrovski, G., Quan, J., Munos, R., and Dabney, W. Recurrent experience replay in distributed reinforcement learning. In *International conference on learning representations*, 2018.
- Kidambi, R., Rajeswaran, A., Netrapalli, P., and Joachims, T. Morel : Model-based offline reinforcement learning. *ArXiv*, abs/2005.05951, 2020.
- Kumar, S., Zamora, J., Hansen, N., Jangir, R., and Wang, X. Graph inverse reinforcement learning from diverse videos. *Conference on Robot Learning (CoRL)*, 2022.

- Kwon, M., Xie, S. M., Bullard, K., and Sadigh, D. Reward design with language models. In *The Eleventh International Conference on Learning Representations*, 2023. URL <https://openreview.net/forum?id=10uNUgI5K1>.
- Lancaster, P., Hansen, N., Rajeswaran, A., and Kumar, V. Modem-v2: Visuo-motor world models for real-world robot manipulation. In *International Conference on Robotics and Automation (ICRA)*, 2024.
- Ma, Y. J., Liang, W., Wang, G., Huang, D.-A., Bastani, O., Jayaraman, D., Zhu, Y., Fan, L., and Anandkumar, A. Eureka: Human-level reward design via coding large language models. *arXiv preprint arXiv: Arxiv-2310.12931*, 2023.
- Memarian, F., Goo, W., Lioutikov, R., Niekum, S., and Topcu, U. Self-supervised online reward shaping in sparse-reward environments. In *2021 IEEE/RSJ International Conference on Intelligent Robots and Systems (IROS)*, pp. 2369–2375. IEEE, 2021.
- Mu, T., Liu, M., and Su, H. Drs: Learning reusable dense rewards for multi-stage tasks. In *The Twelfth International Conference on Learning Representations*, 2024.
- Nair, A., McGrew, B., Andrychowicz, M., Zaremba, W., and Abbeel, P. Overcoming exploration in reinforcement learning with demonstrations. In *2018 IEEE international conference on robotics and automation (ICRA)*, pp. 6292–6299. IEEE, 2018.
- Ng, A. Y., Russell, S., et al. Algorithms for inverse reinforcement learning. In *Icml*, volume 1, pp. 2, 2000.
- Parisi, S., Rajeswaran, A., Purushwalkam, S., and Gupta, A. The unsurprising effectiveness of pre-trained vision models for control, 2022. URL <https://arxiv.org/abs/2203.03580>.
- Peters, J., Mülling, K., and Altün, Y. Relative entropy policy search. In *Proceedings of the Twenty-Fourth AAAI Conference on Artificial Intelligence, AAAI’10*, pp. 1607–1612. AAAI Press, 2010.
- Pomerleau, D. A. Alvin: An autonomous land vehicle in a neural network. In Touretzky, D. (ed.), *Advances in Neural Information Processing Systems*, volume 1. Morgan-Kaufmann, 1988. URL [https://proceedings.neurips.cc/paper\\_files/paper/1988/file/812b4ba287f5ee0bc9d43bbf5bbe87fb-Paper.pdf](https://proceedings.neurips.cc/paper_files/paper/1988/file/812b4ba287f5ee0bc9d43bbf5bbe87fb-Paper.pdf).
- Rajeswaran, A., Kumar, V., Gupta, A., Vezzani, G., Schulman, J., Todorov, E., and Levine, S. Learning complex dexterous manipulation with deep reinforcement learning and demonstrations. *arXiv preprint arXiv:1709.10087*, 2017.
- Rocamonde, J., Montesinos, V., Nava, E., Perez, E., and Lindner, D. Vision-language models are zero-shot reward models for reinforcement learning, 2024. URL <https://arxiv.org/abs/2310.12921>.
- Schaul, T., Quan, J., Antonoglou, I., and Silver, D. Prioritized experience replay, 2016. URL <https://arxiv.org/abs/1511.05952>.
- Schmidhuber, J. *Making the world differentiable: on using self supervised fully recurrent neural networks for dynamic reinforcement learning and planning in non-stationary environments*. Forschungsberichte Künstliche Intelligenz. Inst. für Informatik, 1990. URL <https://books.google.ch/books?id=9c2sHAAACAAJ>.
- Schrittwieser, J., Antonoglou, I., Hubert, T., Simonyan, K., Sifre, L., Schmitt, S., Guez, A., Lockhart, E., Hassabis, D., Graepel, T., Lillicrap, T., and Silver, D. Mastering atari, go, chess and shogi by planning with a learned model. *Nature*, 588(7839):604–609, December 2020. ISSN 1476-4687. doi: 10.1038/s41586-020-03051-4. URL <http://dx.doi.org/10.1038/s41586-020-03051-4>.
- Sferrazza, C., Huang, D.-M., Lin, X., Lee, Y., and Abbeel, P. Humanoidbench: Simulated humanoid benchmark for whole-body locomotion and manipulation, 2024.
- Singh, A., Yang, L., Hartikainen, K., Finn, C., and Levine, S. End-to-end robotic reinforcement learning without reward engineering. *arXiv preprint arXiv:1904.07854*, 2019.
- Smith, L., Dhawan, N., Zhang, M., Abbeel, P., and Levine, S. Avid: Learning multi-stage tasks via pixel-level translation of human videos. *arXiv preprint arXiv:1912.04443*, 2019.
- Smith, L., Dhawan, N., Zhang, M., Abbeel, P., and Levine, S. Avid: Learning multi-stage tasks via pixel-level translation of human videos, 2020. URL <https://arxiv.org/abs/1912.04443>.
- Sutton, R. S. and Barto, A. G. *Reinforcement Learning: An Introduction*. The MIT Press, second edition, 2018. URL <http://incompleteideas.net/book/the-book-2nd.html>.
- Tao, S., Shukla, A., Chan, T.-k., and Su, H. Reverse forward curriculum learning for extreme sample and demonstration efficiency in rl. 2024a.
- Tao, S., Xiang, F., Shukla, A., Qin, Y., Hinrichsen, X., Yuan, X., Bao, C., Lin, X., Liu, Y., kai Chan, T., Gao,

- Y., Li, X., Mu, T., Xiao, N., Gurha, A., Huang, Z., Calandra, R., Chen, R., Luo, S., and Su, H. Maniskill3: Gpu parallelized robotics simulation and rendering for generalizable embodied ai, 2024b. URL <https://arxiv.org/abs/2410.00425>.
- Trott, A., Zheng, S., Xiong, C., and Socher, R. Keeping your distance: Solving sparse reward tasks using self-balancing shaped rewards. *Advances in Neural Information Processing Systems*, 32, 2019.
- Vecerik, M., Sushkov, O., Barker, D., Rothörl, T., Hester, T., and Scholz, J. A practical approach to insertion with variable socket position using deep reinforcement learning. In *2019 international conference on robotics and automation (ICRA)*, pp. 754–760. IEEE, 2019.
- Williams, G., Aldrich, A., and Theodorou, E. Model predictive path integral control using covariance variable importance sampling, 2015. URL <https://arxiv.org/abs/1509.01149>.
- Wu, Z., Lian, W., Unhelkar, V., Tomizuka, M., and Schaal, S. Learning dense rewards for contact-rich manipulation tasks. In *2021 IEEE International Conference on Robotics and Automation (ICRA)*, pp. 6214–6221. IEEE, 2021.
- Xie, A., Singh, A., Levine, S., and Finn, C. Few-shot goal inference for visuomotor learning and planning. In *Conference on Robot Learning*, pp. 40–52. PMLR, 2018.
- Xie, T., Zhao, S., Wu, C. H., Liu, Y., Luo, Q., Zhong, V., Yang, Y., and Yu, T. Text2reward: Reward shaping with language models for reinforcement learning. In *The Twelfth International Conference on Learning Representations*, 2024. URL <https://openreview.net/forum?id=tUM39YTRxH>.
- Yao, Y., Rosasco, L., and Caponnetto, A. On early stopping in gradient descent learning. *Constructive Approximation*, 26:289–315, 2007. URL <https://api.semanticscholar.org/CorpusID:8323954>.
- Yu, T., Thomas, G., Yu, L., Ermon, S., Zou, J. Y., Levine, S., Finn, C., and Ma, T. Mopo: Model-based offline policy optimization. *ArXiv*, abs/2005.13239, 2020.
- Yu, T., Quillen, D., He, Z., Julian, R., Narayan, A., Shively, H., Bellathur, A., Hausman, K., Finn, C., and Levine, S. Meta-world: A benchmark and evaluation for multi-task and meta reinforcement learning, 2021. URL <https://arxiv.org/abs/1910.10897>.
- Zakka, K., Zeng, A., Florence, P., Tompson, J., Bohg, J., and Dwibedi, D. Xirl: Cross-embodiment inverse reinforcement learning. In *Conference on Robot Learning*, pp. 537–546. PMLR, 2022.
- Zhan, A., Zhao, R., Pinto, L., Abbeel, P., and Laskin, M. Learning visual robotic control efficiently with contrastive pre-training and data augmentation, 2022. URL <https://arxiv.org/abs/2012.07975>.
- Zhang, M., Vikram, S., Smith, L., Abbeel, P., Johnson, M. J., and Levine, S. Solar: Deep structured latent representations for model-based reinforcement learning. *ArXiv*, abs/1808.09105, 2018.
- Zhao, R., ufuk topcu, Chinchali, S. P., and Phielipp, M. Accelerating visual sparse-reward learning with latent nearest-demonstration-guided explorations. In *8th Annual Conference on Robot Learning*, 2024. URL <https://openreview.net/forum?id=3NI5SxsJqf>.
- Zhu, Y., Wong, J., Mandlekar, A., Martín-Martín, R., Joshi, A., Nasiriany, S., and Zhu, Y. robosuite: A modular simulation framework and benchmark for robot learning, 2022. URL <https://arxiv.org/abs/2009.12293>.
- Ziebart, B. D., Maas, A. L., Bagnell, J. A., Dey, A. K., et al. Maximum entropy inverse reinforcement learning. In *Aaai*, volume 8, pp. 1433–1438. Chicago, IL, USA, 2008.
- Zolna, K., Novikov, A., Konyushkova, K., Gulcehre, C., Wang, Z., Aytar, Y., Denil, M., de Freitas, N., and Reed, S. Offline learning from demonstrations and unlabeled experience. *arXiv preprint arXiv:2011.13885*, 2020.

## A. Additional Results

### A.1. Single-task Experimental Results

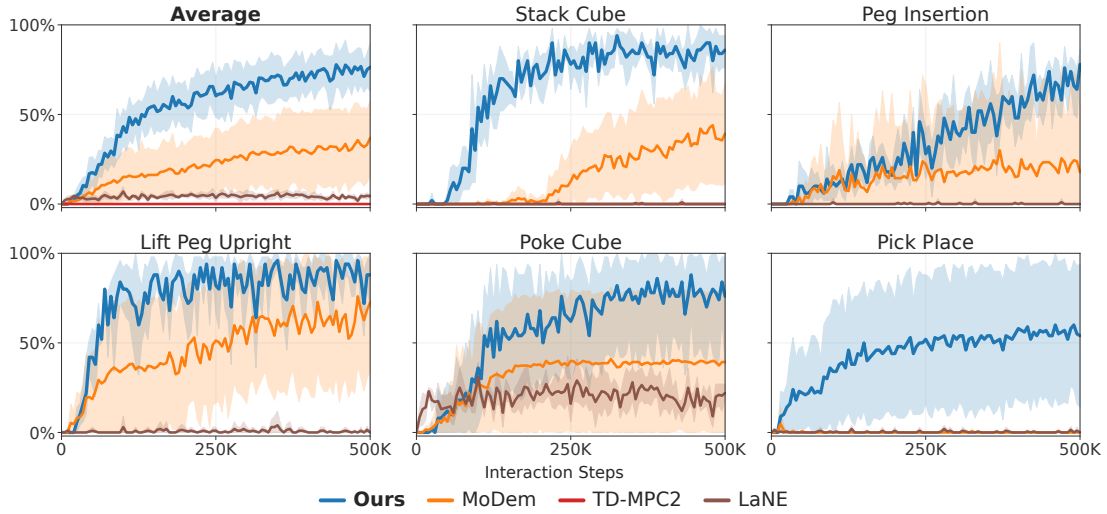


Figure 10. **ManiSkill Manipulation results.** Results averaged across 5 seeds. The shaded area corresponds to a 95% confidence interval.

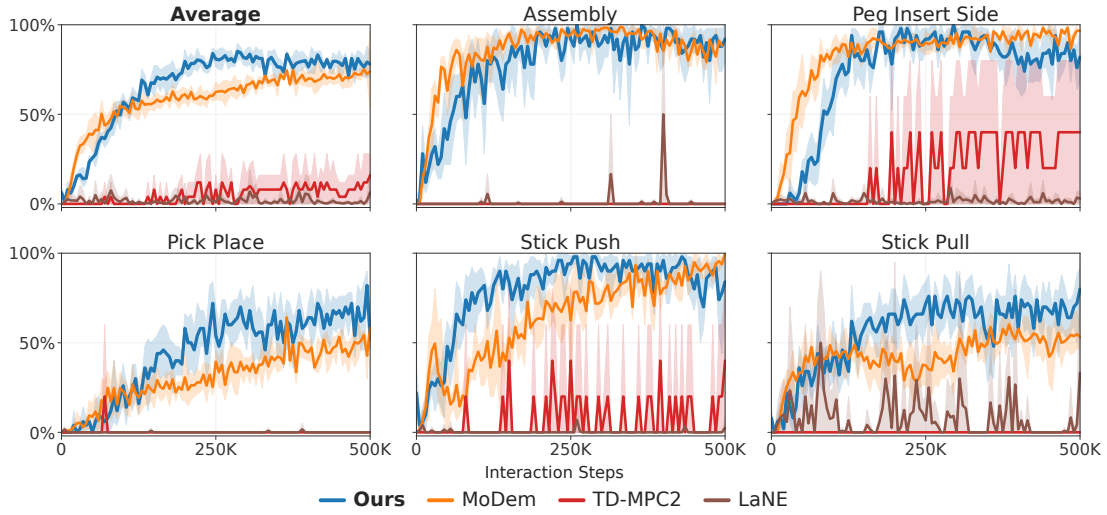


Figure 11. **Meta-World results.** Results averaged across 5 seeds. The shaded area corresponds to a 95% confidence interval.

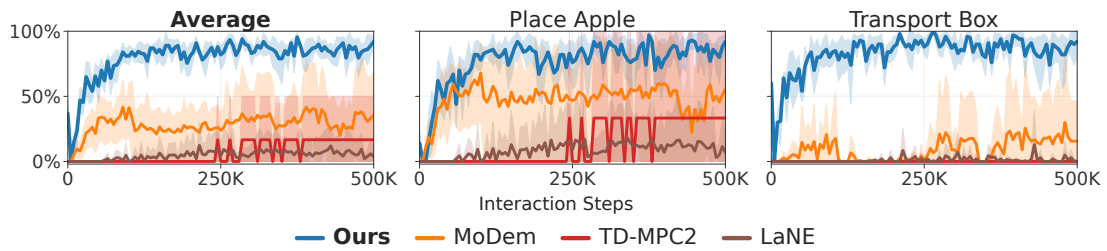


Figure 12. **ManiSkill Humanoids results.** Results averaged across 5 seeds. The shaded area corresponds to a 95% confidence interval.

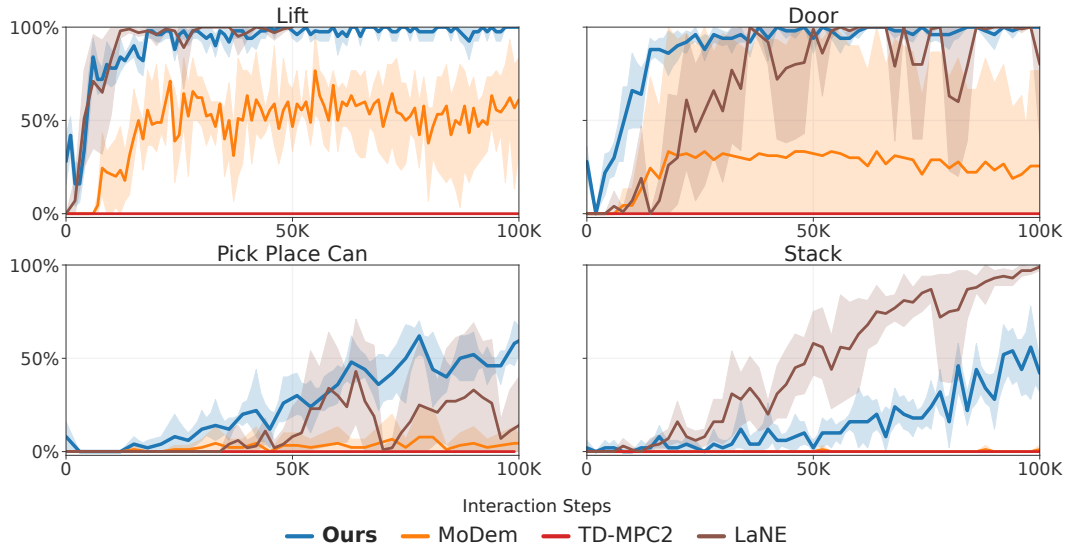


Figure 13. **Robosuite results.** Results averaged across 5 seeds. The shaded area corresponds to a 95% confidence interval.

### A.2. Additional Ablations

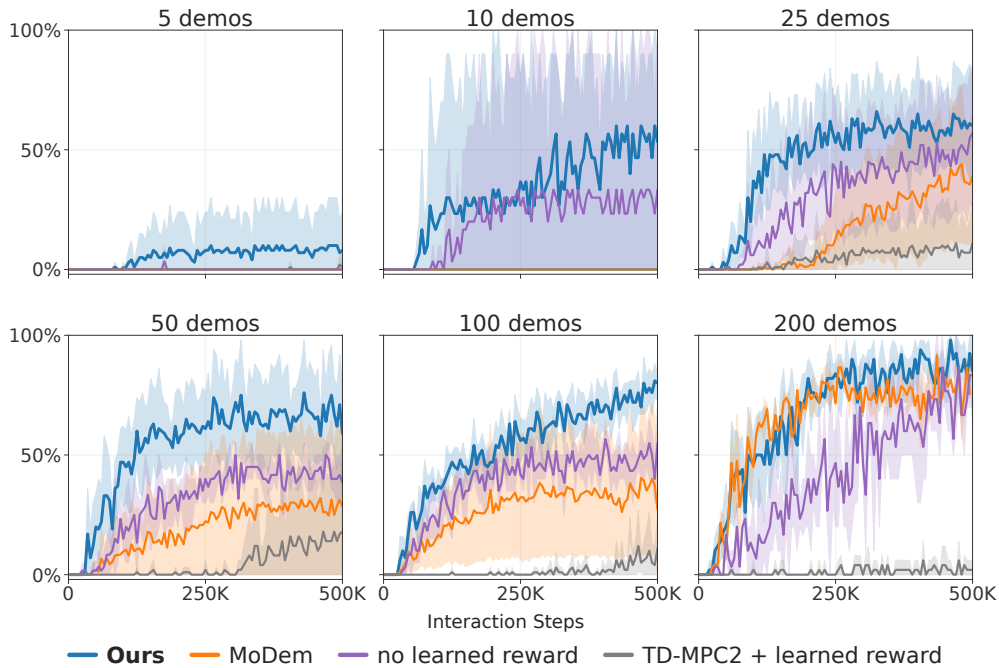


Figure 14. **Demonstration ablation.** Success rate on an increasing number of demonstrations (5-200) in the 2 most challenging manipulation tasks in ManiSkill (Stack Cube and Peg Insertion). DEMO<sup>3</sup> is the only method that has a relative success with only 5 demonstrations. Results are aggregated over both tasks and averaged across 5 seeds.

## B. Baselines

### B.1. Comparison to prior work

In Table 3, we compare key components of DEMO<sup>3</sup> to relevant prior methods on demonstration-augmented RL. Our approach is the only one incorporating online reward learning in multi-stage settings for visual inputs and sparse rewards.

Table 3. **Comparison to prior work.** We compare DEMO<sup>3</sup> to relevant approaches and ablations. Selected baselines are highlighted .

Method	Visual Inputs	Sparse Rewards	Multi-Stage	Online Reward Learning
<b>Ours</b>	✓	✓	✓	✓
LaNE (Zhao et al., 2024)	✓	✓	✗	✓
MoDem (Hansen et al., 2023)	✓	✓	✗	✗
CoDER (Zhan et al., 2022)	✓	✓	✗	✗
SAC + DrS (Mu et al., 2024)	✗	✓	✓	✗
AMP (Escontrela et al., 2022)	✗	✗	✗	✓

### B.2. Baseline Implementations

**TD-MPC2** We use the official implementation<sup>2</sup> with default parameters. We add two extra layers to the convolutional encoders to handle the higher image resolution of the Meta-World and Robosuite benchmarks.

**MoDem** We use the official implementation<sup>3</sup> with default parameters. To process observations containing multiple images, we add an extra encoder to the world model and average all the embeddings.

**LaNE** We use the code from the official implementation<sup>4</sup> with default parameters. To adapt it to our experimental setup, we add extra encoders to handle the additional observations. The proprioceptive state is passed through an MLP, and its embedding is averaged with the other inputs. Additionally, we adapt the algorithm to handle infinite-horizon MDPs by removing value function bootstrapping from the MDP.

<sup>2</sup><https://github.com/nicklashansen/tdmpc2>

<sup>3</sup><https://github.com/facebookresearch/modem>

<sup>4</sup><https://github.com/PhilipZRH/LaNE>

### C. Demonstrations

All of our demonstrations are obtained by training a TD-MPC2 model with dense rewards and state observations. The model trained on state observations is then used to rollout  $N$  episodes in the stage-based environment, from where we query image observations, proprioceptive states, and sparse stage rewards. Please find below a detailed table on the number of demonstrations used per task.

Table 4. **Number of demonstrations for each task.** We use the minimum amount of demonstrations (empirically determined) to ensure that the best-performing algorithm can solve the task in the given interaction budget.

Domain	Task	Number of Demonstrations
ManiSkill Manipulation	<b>Peg Insertion</b>	100
	<b>Pick Place</b>	100
	<b>Stack Cube</b>	25
	<b>Poke Cube</b>	5
	<b>Lift Peg Upright</b>	5
Meta-World	<b>Assembly</b>	5
	<b>Peg Insert Side</b>	5
	<b>Stick Push</b>	5
	<b>Stick Pull</b>	5
	<b>Pick Place</b>	5
ManiSkill Humanoids	<b>Place Apple</b>	5
	<b>Transport Box</b>	5
Robosuite	<b>Lift</b>	5
	<b>Door</b>	10
	<b>Pick Place Can</b>	10
	<b>Stack Blocks</b>	20

## D. Experiment Details

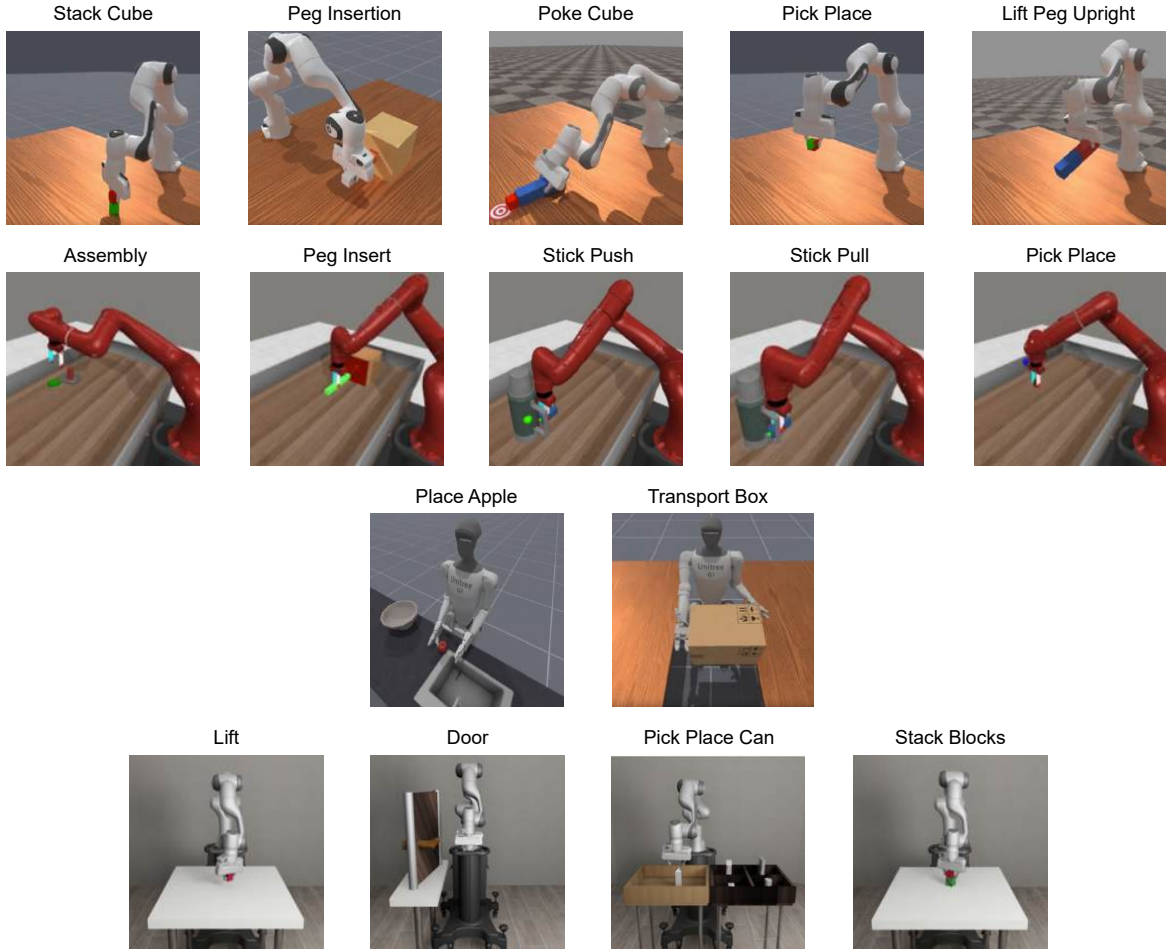


Figure 15. All tasks. Visual description of all tasks organized by domains. In descending order: ManiSkill Manipulation, Meta-World, ManiSkill Humanoids, and Robosuite.

### D.1. Domain Implementation

Table 5. Implementation details for each of our four domains. Time horizon is measured in agent steps (policy forward passes). *Proprio.* stands for Proprioceptive State. Each domain uses different image resolutions according to the detail of the scene.

	ManiSkill Manipulation	Meta-World	ManiSkill Humanoids	Robosuite
<b>Time Horizon</b>	100	100	100	100
<b>Image Size</b>	$128 \times 128$	$224 \times 224$	$128 \times 128$	$128 \times 128$
<b>Observations</b>	RGB(x2) + Proprio.	RGB + Proprio.	RGB(x2) + Proprio.	RGB(x2)
<b>Cameras</b>	Hand + Front	Front	Head + Front	Hand + Front
<b>Action Repeat</b>	2	2	2	1
<b>Action Dim</b>	7	4	25	7



D.2. Stage Definitions

Table 6. ManiSkill Manipulation stage definitions.

Task	Stage 1	Stage 2	Success Criteria
<b>Stack Cube</b>	Red cube grabbed.	Red cube is above green cube.	Red cube is placed on green cube and released.
<b>Peg Insertion</b>	Peg grabbed.	Peg is aligned with hole.	Peg inserted in hole.
<b>Pick Place</b>	Cube grabbed.	Cube is close to goal location.	Cube located at goal position and static.
<b>Poke Cube</b>	Peg grabbed.	Peg is in contact with Cube.	Cube is at goal location.
<b>Lift Peg Upright</b>	Peg grabbed.	Peg is close to upright position.	Peg is in the upright position on the desk.

Table 7. Meta-World stage definitions.

Task	Stage 1	Success Criteria
<b>Assembly</b>	Grab hook.	Pass nut through pole.
<b>Peg Insert</b>	Peg grabbed.	Peg inserted in hole.
<b>Stick Push</b>	Stick grabbed.	Object pushed to goal location.
<b>Stick Pull</b>	Stick grabbed.	Object pulled to goal location.
<b>Pick Place</b>	Cube grabbed.	Cube is static at goal.

Table 8. ManiSkill Humanoids stage definitions.

Task	Stage 1	Stage 2	Success Criteria
<b>Place Apple</b>	Apple is grabbed.	Apple is above bowl.	Apple is inside bowl.
<b>Transport Box</b>	Box grabbed with 2 hands.	Box above table 2.	Box is on table 2.

Table 9. Robosuite stage definitions.

Task	Success Criteria
<b>Lift</b>	Block lifted above the desk.
<b>Door</b>	Door is open.
<b>Pick Place Can</b>	Can is at goal location.
<b>Stack</b>	Block A is in contact with Block B and above the ground.

### D.3. Difficulty Categorization

Across this paper, we often refer to some tasks as more *difficult* than others. To characterize task difficulty, we follow (Tao et al., 2024a). As in previous work on demonstration-augmented reinforcement learning (RL), we observe that environments with high complexity and substantial initial state randomization are typically more difficult to solve and require a larger number of demonstrations. For example, the *Peg Insertion* task from *ManiSkill* exhibits significant variability in the peg’s position, orientation, and the hole’s size. Consequently, around 100 demonstrations are needed to solve the task from visual inputs. In contrast, a task like *Meta-World Assembly* requires only 5 demonstrations to be successfully solved. Figure 16 qualitatively compares the different initial states of these two tasks. We hypothesize that this effect is related to the distributional coverage of the demonstration dataset: higher randomization reduces the likelihood that the agent encounters familiar states during training if the dataset is limited. Therefore, as the variability in a task’s initial state increases, this variability must also be well-represented in the dataset to ensure effective learning.

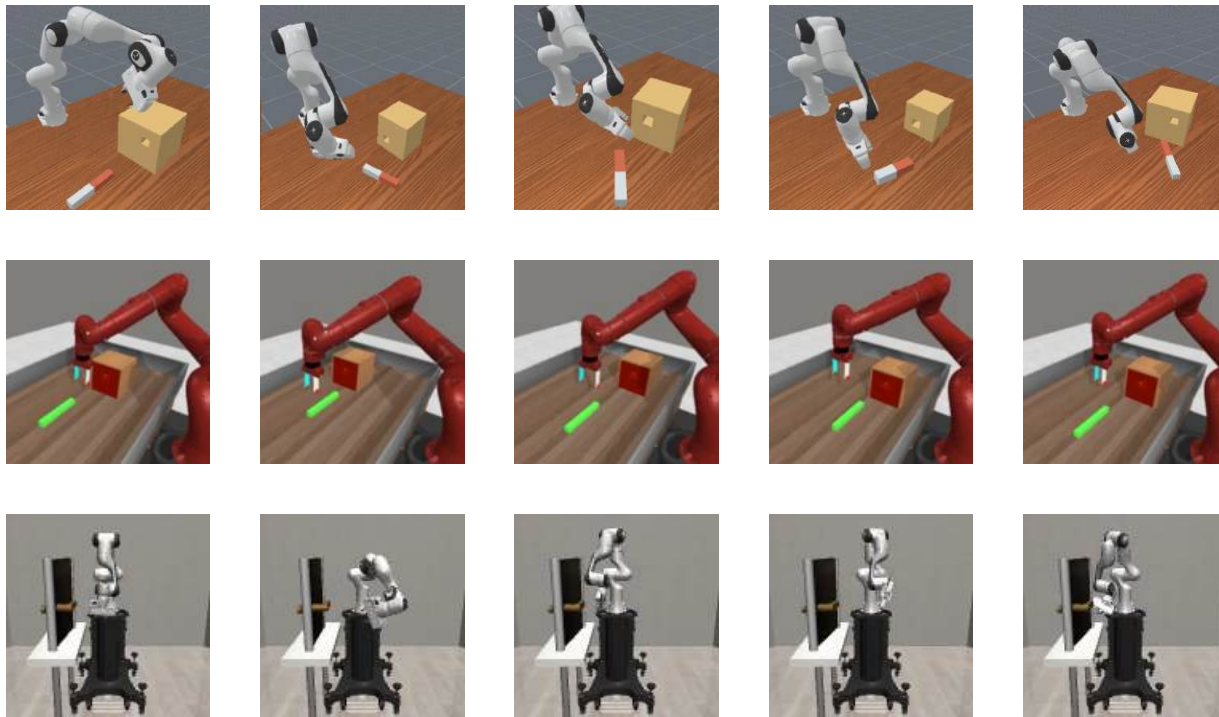


Figure 16. **Randomization comparison.** Qualitative comparison of both Peg Insertion tasks in the ManiSkill and Meta-World domain and Door task in Robosuite. Visibly, ManiSkill presents the highest level of randomization, not only varying the initial state at reset but also changing the geometric properties of the objects.

## E. Implementation Details

### E.1. Model Architecture

Following TD-MPC2, all modules are implemented as MLPs. Here, as an example, we summarize our architecture for a single-camera Meta-World task using PyTorch-like notation:

```

Architecture: TD-MPC2 World Model
Encoder: ModuleDict(
  (rgb_frontview): Sequential(
    (0): ShiftAug()
    (1): PixelPreprocess()
    (2): Conv2d(3, 32, kernel_size=(7, 7), stride=(2, 2))
    (3): ReLU(inplace=True)
    (4): Conv2d(32, 32, kernel_size=(5, 5), stride=(2, 2))
    (5): ReLU(inplace=True)
    (6): Conv2d(32, 32, kernel_size=(3, 3), stride=(2, 2))
    (7): ReLU(inplace=True)
    (8): Conv2d(32, 32, kernel_size=(3, 3), stride=(2, 2))
    (9): ReLU(inplace=True)
    (10): Conv2d(32, 32, kernel_size=(3, 3), stride=(1, 1))
    (11): Flatten(start_dim=1, end_dim=-1)
    (12): Linear(in_features=512, out_features=512, bias=True)
    (13): SimNorm(dim=8)
  )
)
Dynamics: Sequential(
  (0): NormedLinear(in_features=519, out_features=512, bias=True, act=Mish)
  (1): NormedLinear(in_features=512, out_features=512, bias=True, act=Mish)
  (2): NormedLinear(in_features=512, out_features=512, bias=True, act=SimNorm)
)
Reward: Sequential(
  (0): NormedLinear(in_features=519, out_features=512, bias=True, act=Mish)
  (1): NormedLinear(in_features=512, out_features=512, bias=True, act=Mish)
  (2): Linear(in_features=512, out_features=101, bias=True)
)
Policy prior: Sequential(
  (0): NormedLinear(in_features=512, out_features=512, bias=True, act=Mish)
  (1): NormedLinear(in_features=512, out_features=512, bias=True, act=Mish)
  (2): Linear(in_features=512, out_features=14, bias=True)
)
Q-functions: Vectorized [Sequential(
  (0): NormedLinear(in_features=519, out_features=512, bias=True, dropout=0.01, act=Mish)
  (1): NormedLinear(in_features=512, out_features=512, bias=True, act=Mish)
  (2): Linear(in_features=512, out_features=101, bias=True)
), Sequential(
  (0): NormedLinear(in_features=519, out_features=512, bias=True, dropout=0.01, act=Mish)
  (1): NormedLinear(in_features=512, out_features=512, bias=True, act=Mish)
  (2): Linear(in_features=512, out_features=101, bias=True)
), Sequential(
  (0): NormedLinear(in_features=519, out_features=512, bias=True, dropout=0.01, act=Mish)
  (1): NormedLinear(in_features=512, out_features=512, bias=True, act=Mish)
  (2): Linear(in_features=512, out_features=101, bias=True)
)]
Learnable parameters: 5,448,748
Discriminator Architecture: Discriminator(
  (nets): ModuleList(
    (0): Sequential(
      (0): Linear(in_features=512, out_features=32, bias=True)
      (1): Sigmoid()
      (2): Linear(in_features=32, out_features=1, bias=True)
    )
  )
)

```

E.2. Hyperparameters

Most of the hyperparameters remain unchanged from our backbone algorithm, TD-MPC2. Here, we list some of the most relevant to our method and highlight the ones that are unique to our approach. Please refer to the TD-MPC2 paper (Hansen et al., 2024) for a complete list of hyperparameters.

Table 10. Hyperparameters used in the training setup.

Hyperparameter	Value
<b>Replay buffer</b>	
Capacity	300,000
Sampling	Uniform
<b>Architecture (5M)</b>	
Encoder arch.	ConvNet (image inputs) MLP (state inputs)
Conv. layers	7 (Meta-World) 5 (Otherwise)
Encoder MLP dim	256
Dynamics MLP dim	512
Latent state dim	512
Task embedding dim	96
<b>Optimization</b>	
Update-to-data ratio	1
Batch size	256
Joint-embedding coef.	20
Reward prediction coef.	0.1
Value prediction coef.	0.1
Temporal coef. ( $\lambda$ )	0.5
Q-fn. momentum coef.	0.99
Policy prior entropy coef.	$1 \times 10^{-4}$
Policy prior loss norm.	Moving (5%, 95%) percentiles
Optimizer	Adam
Learning rate	$3 \times 10^{-4}$
Encoder learning rate	$1 \times 10^{-4}$
<b>Pretraining</b>	
Pretraining loss	Behavioral cloning
BC Policy Architecture	MLP
MLP dim	512
Optimizer	Adam
Learning rate	$3 \times 10^{-4}$
Encoder learning rate	$3 \times 10^{-4}$
Initial pretrained action ratio $\alpha_0$	$5 \times 10^{-5}$
<b>Reward learning</b>	
Discriminator architecture	MLP
MLP dim	32
Discriminator learning rate	$3 \times 10^{-4}$
Discriminator optimizer	Adam
Batch size	256
Learned reward coefficient $\beta$	1/3
Demo. sampling ratio	50%

### **E.3. Computational Resources**

All our experiments run in a single NVIDIA GeForce RTX 3090 GPU and 32GB of RAM to store collected samples.